L07

Proceedings of the 5th International Conference on Inverse Problems in Engineering : Theory and Practice, Cambridge, UK, 11-15th July 2005

CHARACTERIZATION OF THERMAL CONTACT CONDUCTANCE DURING RESISTANCE SPOT WELDING

T. LOULOU, P. LE MASSON and P. ROGEON
Université de Bretagne Sud, Centre de Recherche LET2E, F-56321, Lorient, France
e-mail: tahar.loulou@univ-ubs.fr

Abstract - This work discusses parameter estimation techniques in recovering the thermo-physical parameters which characterize the thermal behavior of two solids in combined thermal and electrical contact. It consists in estimating simultaneously the heat flux released at the interface, the partition coefficient of this heat flux, and the thermal contact conductance between the two solids. The estimation problem was formulated as an inverse problem which aims minimizing the square difference between the measured and computed temperatures in the neighborhood of the contact interface. The present parameter estimation problem is solved with the Levenberg-Marquardt method to estimate simultaneously the three unknowns of the interface. A detailed analysis of the linear dependency of the contact parameters needed to design a robust estimation tool is presented. In order to perform this analysis, the sensitivity coefficients and the sensitivity matrix determinant were carefully examined. Simulated temperature measurements were obtained from the solution of the direct problem by prescribing *a priori* known parameters. Despite strong correlation between the generated heat flux and its partition coefficient, the results show that the estimation is feasible and the developed method is an effective tool in complete thermal characterization of the contact interface.

1. INTRODUCTION

Resistance spot welding is a joining process in which flat surfaces are joined in one or more spots by the heat generated by resistance to the flow of electric current through work-pieces that are held together under force by electrodes. The contacting surfaces in the region of current concentration are heated by short time pulses of low voltage, high amperage current to form a fused nugget of weld metal. When the flow of current ceases, the electrode force is maintained while the weld metal rapidly cools and solidifies. The electrodes are retracted after each weld cycle. From the above brief description we can conclude that the main process variables are welding current, current time, electrode force, and electrode characteristics. The current is concentrated at the joining point using cylindrical electrodes having spherical tips. The resistance welding processes employ a combination of mechanical force and heat generation to produce a weld between the work-pieces. More technical details of this joining process are given in many metal-working and manufacturing process books [1]. A schematic representation of resistance spot welding is given in Figure 1. Also, thermal circuit at the joining axis and a whole welding cycle are shown on this figure.

The welding current, electrode force, and weld time can be easily measured, but the different resistances, occurring in the bodies and at the contact interfaces, are complex factors and difficult to measure. The global resistance that is very important in resistance spot welding, is composed of several parts shown on Figure 1, ***see Thermal circuit*** : (1) the contact resistance between the work-pieces (where the melt occurs) $\mathcal{R}_1$, (2) the body resistance of work-pieces $\mathcal{R}_2$, (3) the contact resistances between the electrodes and the work-pieces $\mathcal{R}_3$, and (4) the body resistance of the electrodes $\mathcal{R}_4$. During spot resistance welding, temperatures in the bodies should be controlled within precise limits in order to achieve the desired mechanical and metallurgical properties of welded pieces. In the goal to predict precisely the transient temperature distribution and the resultant welding quality of sheets, the heat transfer coefficient $h(t)$ at the electrode work-pieces interface is required and should be carefully investigated. This coefficient characterizes the third resistance cited above : $h(t) = 1/\mathcal{R}_3(t)$.

As it has been mentioned in several references [5, 12], thermal contact resistance has great importance in the enhancement or the reduction of the heat transfer at the interface of two elements in contact. This parameter is greatly affected by the physical conditions of the contact such as : surface cleanliness and freedom oxides or other chemical compounds, the roughness or smoothness of the surfaces in contact, the joining force, level of temperature contact, thermophysical properties of materials in contact, etc.

Indeed, thermal contact conductance undergoes a big change when one of the bodies in contact is involved in hard mechanical and thermal conditions. During this process, the electrodes work-pieces contact makes a transition from a dry solid-solid metal contact to a solid-soft metal contact. This transition period must be identified and investigated in the goal to be more accurate and realistic in any thermal analysis of the spot welding process.

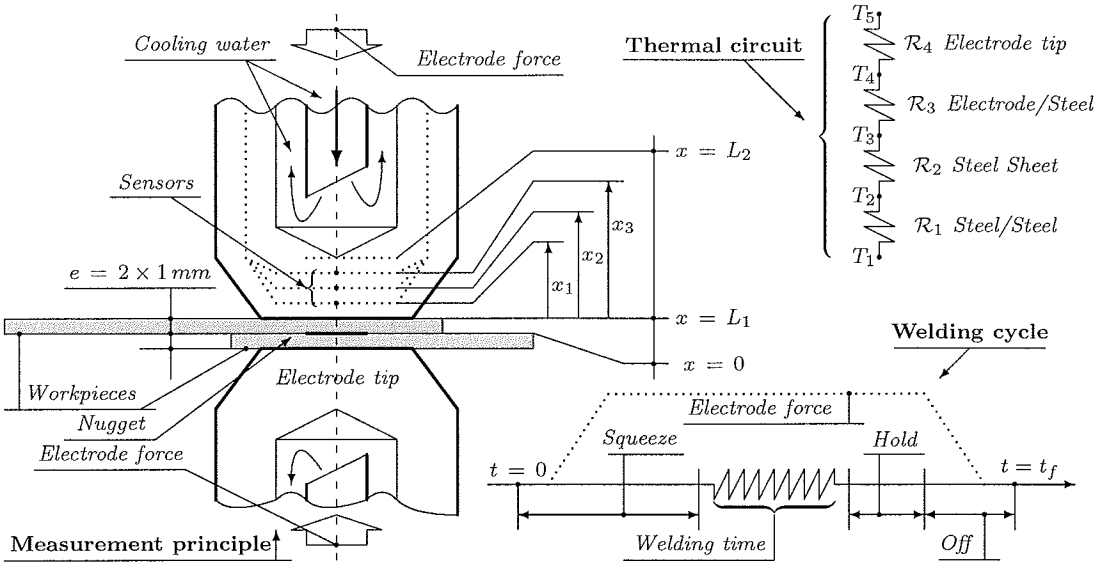

Figure 1. Schematic representation of resistance spot welding, thermal circuit and welding cycle.

In the case of combined thermal and electrical contact, moreover the classical thermal contact conditions characterized by the temperature jump and the heat flux continuity conditions at the interface, two additional unknowns should be taken into account. The first unknown is the generated heat flux (by Joule effect) at the contact interface resulting from the imperfect electrical contact at the interface. The second unknown is the partition coefficient that rules the heat flux sharing between the two regions in contact, i.e. the electrode tip and the metal sheet. The introduction and definition of this concept takes its roots in the early sixties of the last century when several authors initiated the study of this problem. This problem is encountered in many cases such as sliding, rolling, electrical connectors, brake, skiing, etc [4,6,7,9,16]. A whole thermal characterization of the interface needs the knowledge of its three governing parameters : generated heat flux q, the partition coefficient a, and the thermal contact conductance h. In recent work, Le Meur [10] has encountered some difficulties in estimating a and h as two constants parameters. In his analysis, he shows a big linearity between a and h which leads to a difficult estimation. A similar work, but with an application to sliding contact was performed by Bauzin [2].

In this work, the same model as Le Meur's one is used but with different approaches. The first one consists in formulating the problem in dimensionless variables which makes the analysis more universal and the comparison more effective. The second one consists in using in-situ temperature measurements. In other words, temperature profiles needed for the estimation are generated during a whole simulated welding cycle starting at room temperature in both regions. As third approach, our parameter estimation problem is solved with the Levenberg-Marquardt method to estimate simultaneously the three thermal unknowns of the interface. A detailed analysis of the linear dependency of the contact parameters needed to design a robust estimation tool is presented. In order to perform this analysis, the sensitivity coefficients and the sensitivity matrix determinant were carefully examined during a complete welding cycle.

The structure of this paper is as follows. Experimental setup and measurement principle of contact parameter is described briefly in the first section. The statement and formulation of the transient direct and inverse problems is given in the second section. Then the estimation and its feasibility is detailed in the third section. Numerical results and discussion are given in the fourth section. Finally, a summary and conclusion in presented in the last section.

2. TEMPERATURE MEASUREMENTS

The main idea of the experimental setup was the development of a fine thermal metrology, incorporated in the electrode tip and the steel sheet and which is able to record temperature histories during the welding process. This instrumentation must be robust and efficient in such hard thermal, mechanical and electrical environment and able to minimize the disturbance of the measurements induced by the sensor presence and the high electric noise. A detailed representation of the experimental device is given in Figure 1. A complete description of the experimental facilities are well described and detailed in reference [11]. The fundamental idea behind such experimental work

is the collection of temperature histories in the electrode tip evolving in physical conditions as close as possible to real world of welding. This experimental approach enables a thermal characterization of the dynamic contact in the welding process.

3. DIRECT PROBLEM FORMULATION

Looking to the symmetry of the geometrical configuration, and the small distances, the problem of estimating the three parameters characterizing the contact interface in spot welding can be formulated in half region representing one electrode tip and one work-piece using one-dimensional heat transfer approach. See Figure 1. For the most accurate modeling of the welding process, the phase-change effects taking place in the workpieces should be included in the model. However, for generality in this study and the sake of brevity and simplicity of the model, the phase change effects are not included here.

Then the two solids, referred to as regions 1 and 2, are in thermal contact with the quantities $q_2(t)$, a, and h being respectively the heat flux generated at the interface, the partition coefficient of this heat flux between solid 1 and 2, and the thermal contact conductance. One of the non-contacting ends dissipate heat by convection into one fluid at temperature T_∞ with heat transfer coefficients h_2 while the second one is subjected to an applied heat flux $q_1(t)$. The mathematical formulation of this heat conduction problem, with constant thermophysical properties, is given in dimensionless form for region 1 as follow :

$$\frac{\partial T_1(x,t)}{\partial t} = \frac{\partial^2 T_1(x,t)}{\partial x^2} + S_1(t) \qquad 0 < x < 1, \qquad t > 0 \tag{1}$$

$$T_1(x,t) = 0 \qquad 0 \le x \le 1, \qquad t = 0 \tag{2}$$

$$-\frac{\partial T_1(x,t)}{\partial x} = q_1(t) \qquad x = 0, \qquad t > 0 \tag{3}$$

$$+\frac{\partial T_1(x,t)}{\partial x} = (1-a)q_2(t) + h\left[T_2(x,t) - T_1(x,t)\right] \qquad x = 1, \qquad t > 0 \tag{4}$$

for region 2 ($1 < x < 1 + L$) as

$$\frac{1}{\alpha}\frac{\partial T_2(x,t)}{\partial t} = \frac{\partial^2 T_2(x,t)}{\partial x^2} + \frac{S_2(t)}{k} \qquad 1 < x < 1+L, \qquad t > 0 \tag{5}$$

$$T_2(x,t) = T_2^i \qquad 0 \le x \le 1+L, \qquad t = 0 \tag{6}$$

$$-k\frac{\partial T_2(x,t)}{\partial x} = aq_2(t) + h\left[T_1(x,t) - T_2(x,t)\right] \qquad x = 1+L, \qquad t > 0 \tag{7}$$

$$-k\frac{\partial T_2(x,t)}{\partial x} = h_2\left[T_2(x,t) - T_\infty\right] \qquad x = 1+L, \qquad t > 0 \tag{8}$$

where the following dimensionless quantities were defined :

$$x = \frac{\bar{x}}{\bar{L}_1} \qquad t = \frac{\bar{\alpha}_1 \bar{t}}{\bar{L}_1^2} \qquad \alpha = \frac{\bar{\alpha}_2}{\bar{\alpha}_1} \qquad k = \frac{\bar{k}_2}{\bar{k}_1} \qquad L = \frac{\bar{L}_2}{\bar{L}_1} \qquad q = \frac{\bar{q}}{\bar{q}_r} \qquad Q = \frac{\bar{Q}}{\bar{q}_r}$$

$$h = \frac{\bar{h}\,\bar{L}_1}{\bar{k}_1} \qquad h_2 = \frac{\bar{h}_2\,\bar{L}_1}{\bar{k}_1} \qquad T_1 = \frac{\bar{T}_1 - \bar{T}_1^i}{\bar{q}_r\bar{L}_1/\bar{k}_1} \qquad T_2 = \frac{\bar{T}_2 - \bar{T}_1^i}{\bar{q}_r\bar{L}_1/\bar{k}_1}$$

$$T_2^i = \frac{\bar{T}_2^i - \bar{T}_1^i}{\bar{q}_r\bar{L}_1/\bar{k}_1} \qquad T_\infty = \frac{\bar{T}_\infty - \bar{T}_1^i}{\bar{q}_r\bar{L}_1/\bar{k}_1} \qquad S_1(t) = \frac{\sigma_1 J^2 \bar{L}_1}{\bar{q}_r} \qquad S_2(t) = \frac{\sigma_2 J^2 \bar{L}_1}{\bar{q}_r}$$

and where $\bar{q}_r$ is a reference value for the generated heat flux at the interface, σ_i is the electrical resistivity of the medium i, and J represents the current density flowing in both regions. In the above system, the temperature is made dimensionless by a group containing the heat flux $\bar{q}_r\bar{L}_1/\bar{k}_1$ to remove the dependence on the heat flux magnitude. Consequently, as will be discussed later in this paper, the optimal conditions depend only on the sensor location, dimensionless heating time, and experiment duration.

By following the same approach developed in references [10, 11], the generated heat fluxes $q_1(t)$ and $q_2(t)$ at $x = 0$ and $x = 1$ and the volumetric sources $S_1(t)$ and $S_2(t)$ in region (1) and (2) follow the form of a step function in time, i.e.

$$q_1(t) = \begin{cases} Q, & \text{for } 0 < t \le t_h \\ 0, & \text{for } t > t_h \end{cases} \qquad q_2(t) = \begin{cases} q, & \text{for } 0 < t \le t_h \\ 0, & \text{for } t > t_h \end{cases} \qquad S_i(t) = \begin{cases} G_i, & \text{for } 0 < t \le t_h \\ 0, & \text{for } t > t_h \end{cases} \tag{9}$$

where the quantities Q, q, and G_i $(i = 1, 2)$ are assumed to be constant over the heating time interval $[0,\ t_h]$ which corresponds to the duration of the current flow through the different pieces, i.e. electrodes and workpieces. Indeed, the generated heat is due mainly to the joule effect taking place in the two solids and their common interface during the short current flow.

In the direct problem associated with the physical problem described above, the dimensionless thermophysical properties α, k, the heat transfer coefficients h, h_2, as well as the heat flux generated at the interface $q_2(t)$ and its partition coefficient a, the initial and external temperatures T_1^i, T_2^i, T_∞ and the boundary condition $q_1(t)$ are known. The objective of the direct problem is then to determine the transient temperature field in the two regions resulting from the heat generated in two regions and at the contact interface.

4. INVERSE PROBLEM FORMULATION

The inverse problem considered here is concerned with the estimation of three constant parameters defined by the following vector $\mathbf{U}^T = [a,\ h,\ q]$, from the knowledge of transient temperature measurements taken at some locations inside the two bodies in contact. We suppose that the transient temperature recordings are measured at N_s sensor locations $1 < x_i < 1 + L$, $i = 1, \ldots N_s$. Here N_s designates the temperature sensor number which are installed in the electrode side as shown in Figure 1.

The inverse problem formulated above can be regarded as an optimization problem which aims at finding the unknown thermal property vector $\mathbf{U}^T = [a,\ h,\ q] = [u_1,\ u_2,\ u_3]$ (the superscript T denotes transpose). The basic process involves the minimization of the ordinary least squares norm defined as follow :

$$S(\mathbf{U}) = \sum_{i=1}^{N_s} \sum_{j=1}^{N_t} \left[T(x_i, t_j) - Y(x_i, t_j)\right]^2 \tag{10}$$

where $T(x_i, t_j)$ and $Y(x_i, t_j)$ are respectively the computed and measured temperature at the sensor locations x_i, $i = 1, \ldots N_s$ and different time t_j, $j = 1, \ldots N_t$. Several minimization techniques can be applied to minimize the function (10) [3, 14, 15]. In vectorial form, the above expression can be written as

$$S(\mathbf{U}) = \left[\mathbf{Y} - \mathbf{T}(\mathbf{U})\right]^T \left[\mathbf{Y} - \mathbf{T}(\mathbf{U})\right] \tag{11}$$

To determine the thermal properties of interest the function $S(\mathbf{U})$ is minimized with respect to each component of the vector $\mathbf{U}$. This is accomplished by first setting the derivative of $S(\mathbf{U})$ with each parameter equal to zero, and second linearizing the obtained results which gives the well known Gauss-Newton method [3, 14].

Various modifications of the Gauss-Newton are given in the literature [3] and one modified version of this method is considered in this study. This is the Levenberg-Marquardt method which is given by the following iterative scheme :

$$\mathbf{U}^{(k+1)} = \mathbf{U}^{(k)} + \left[(\mathbf{X}^{(k)})^T(\mathbf{X}^{(k)}) + \mu^{(k)}\mathbf{\Omega}^{(k)}\right]^{-1} (\mathbf{X}^{(k)})^T \left[\mathbf{Y} - \mathbf{T}(\mathbf{U}^{(k)})\right] \tag{12}$$

where the superscript (k) defines the iteration number and $\mathbf{X}$ represents the sensitivity matrix evaluated at the iteration (k). The coefficient $\mu^{(k)}$ is a positive scalar named damping parameter, $\mathbf{\Omega}^{(k)}$ is a diagonal matrix. The purpose of of the matrix term $\mu^{(k)}\mathbf{\Omega}^{(k)}$ is to damp oscillations and instabilities due to the ill-conditioned character of the problem. In explicit form, the sensitivity matrix is given by :

$$\mathbf{X} = \left[\frac{\partial \mathbf{T}^T(\mathbf{U})}{\partial \mathbf{U}}\right]^T = \begin{bmatrix} \dfrac{\partial T_1}{\partial u_1} & \cdots & \dfrac{\partial T_1}{\partial u_3} \\ \vdots & \ddots & \vdots \\ \dfrac{\partial T_N}{\partial u_1} & \cdots & \dfrac{\partial T_N}{\partial u_3} \end{bmatrix} \tag{13}$$

where $N = N_s \times N_t$. The sensitivity matrix coefficients can provide considerable insight into the estimation problem and in the design of the experiment for optimum accuracy in the estimates.

Iterations continue until convergence of the estimated parameter is reached, i.e. when there is negligible change in any component of $\mathbf{U}$. One of various stopping criteria, developed in the literature, to accomplish iterations is defined as follow :

$$\frac{|\ \mathbf{U}^{(k+1)} - \mathbf{U}^{(k)}\ |}{|\mathbf{U}^{(k+1)}|} \leq \varepsilon \tag{14}$$

where ε is a small number which is used to quantify the convergence, eg 10^{-5}.

5. SENSITIVITY COEFFICIENTS AND EXPERIMENTAL DESIGN

The elements of the sensitivity matrix are the sensitivity coefficients [3]. Prior to performing the inverse analysis of identifying the thermal properties of the interface, it is useful to compute the sensitivity coefficients as functions of time. They are defined as the first derivative of measured quantities, i.e. the temperature, with respect to each of the unknown parameters u_i, $i = 1, \ldots, N_p$, where N_p is the number of parameters. They provide valuable insight into how well-designed is the experiment [3]. In general, the sensitivity coefficient are desired to be uncorrelated, i.e. linearly independent.

In problems involving parameters with different orders of magnitude, which is the situation in this problem, the sensitivity coefficients with respect to the various parameters may also differ by several orders of magnitude, creating difficulties in their comparison and identification of linear dependance. These kinds of difficulties can be alleviated through the analysis of the reduced coefficients, which are obtained by multiplying the original sensitivity coefficients by the parameters that are referred to. Several ways can be used to compute these coefficients [3,14]. In our case, the sensitivity coefficients are computed by central finite-difference as follows :

$$X_{ijk} = u_j \frac{T(x_k, t_i, u_1, \ldots, u_j + \varepsilon u_j, \ldots, u_{N_p}) - T(x_k, t_i, u_1, \ldots, u_j - \varepsilon u_j, \ldots, u_{N_p})}{2\,\varepsilon\, u_j} \tag{15}$$

where $\varepsilon = 10^{-5}$ is a small perturbation of the corresponding parameter.

The design of the optimum experiments is of great importance in parameter and/or function estimations. Optimal experiment means the definition of the conditions under which an experiment is to be performed in order to maximize the accuracy with which the results are obtained. Based on the concepts described in references [3] and [14], we choose the optimal duration of the experiment by considering available for the inverse analysis a large but fixed number of measurements, of three sensors ($N_s = 3$) located at x_1, x_2, and x_3 in the electrode tip in the vicinity of the interface as shown in Figure 1. We also take into account the maximum temperature reached in the two regions (sheet and electrode), T_m, obtained from the solution of the direct problem at each final time considered. Hence, we choose to maximize the determinant Δ of the matrix $\mathbf{X}^T\mathbf{X}$, the elements of which are defined by the following expression [3, 14] :

$$C_{ij} = \frac{1}{N_s\, t_f} \sum_{k=1}^{N_s} \int_0^{t_f} \left[u_i \frac{\partial T_k}{\partial u_i}\right] \left[u_j \frac{\partial T_k}{\partial u_j}\right] \left[\frac{1}{T_m}\right]^2 dt \tag{16}$$

where the subscripts i and j refer to the matrix row and column, respectively ($i, j = 1, 2, 3$). This experimental design scheme is based on the so-called D-optimum design which consists in minimizing the confidence region of the estimated parameters.

6. STATISTICAL ANALYSIS

Once the minimization of the least square norm is accomplished, a statistical analysis should be performed in order to evaluate confidence intervals and a confidence region for the estimated parameters [3]. Confidence intervals at the 99 % confidence level are obtained as

$$\bar{u}_j - 2.576\sigma_{\bar{u}_j} \leq \bar{u}_j \leq \bar{u}_j + 2.576\sigma_{\bar{u}_j} \qquad j = 1, \ldots, N_p \tag{17}$$

where the components $\bar{u}_j$ are the value estimated for the unknown parameters, u_j, for $j = 1, \ldots, N_p$, and $\sigma_{\bar{u}_j}$ are the standard deviation obtained from the covariance matrix of the estimated parameters. The confidence region can be computed from, namely

$$\left[\bar{\mathbf{U}} - \mathbf{U}\right]^T \left[\left[\mathbf{X}^T\mathbf{X}\right]^{-1}\sigma^2\right]^{-1} \left[\bar{\mathbf{U}} - \mathbf{U}\right] \leq \chi^2_{N_p} \tag{18}$$

where $\chi^2_{N_p}$ is the chi-square distribution for N_p degrees of freedom, for a given confidence level, and the matrix $\left[\mathbf{X}^T\mathbf{X}\right]^{-1}\sigma^2$ represents the covariance matrix of the estimated parameters [3, 14].

7. RESULTS AND DISCUSSION

From a physical point of view, it is clear that taking a, h, and q as three constants is far from the real thermal problem, that evolves at the interface. Indeed, the three quantities are strongly time dependent functions, or even temperature dependent functions. By considering the welding cycle presented in Figure 1, a first approximation about the time evolution of a, h, and q can be drawn. At the start of the cycle, the contact quality is poor and

this makes the heat coefficient h very weak, while the heat flux q is very important due to the high electrical contact resistance at the interface. At the end of the welding cycle, the above remarks are completely inverted. The generated heat in the electrode-workpieces reduces the metal hardness and as a consequence, the contact quality enhances, the heat transfer coefficient upgrades and the generated heat flux decreases. This reduction in growth of heat flux results from the weakness of the interface to the current flow in the first step, and the cessation of heating in the second one when the time t becomes greater than t_h. The theoretical results presented in reference [10] show a constant behavior of a during all the welding cycle. This model was contradicted in the same reference when experimental data were used in estimating simultaneously a and h. The author shows a decrease of a instead of a constant time evolution.

In the remaining part of this paper, we consider a, h, and q as three constants to demonstrate : (1) the best experimental conditions essential for an accurate estimation, (2) the possibility of using the temperature histories recorded in the electrode body, during welding as additional information for the inverse analysis, (3) the nonlinear dependence between the parameters, and (4) the feasibility of the simultaneous estimation of these parameters.

The present parameter estimation problem is known as nonlinear, because the sensitivity coefficients are functions of the unknowns parameters. As a result, the analysis of the sensitivity coefficients and the determinant of the matrix $\mathbf{X}^T\mathbf{X}$ presented below is not global, that is, it is dependent on the values chosen in advance for the unknown parameters. Let us consider in this paper a test case involving the following reference values for the dimensionless variables : $a = 0.50$, $h = 22.22$, and $q = 0.89$. This case corresponds to the welding parameters of two steel sheets with two copper electrode tips [10].

Figure 2 shows typical temperature profiles measured at three sensor locations in the electrode tip after adding a white noise to the exact values. Figures 3, 4, and 5 present respectively the time evolution of the reduced sensitivity coefficients X_a, X_h, and X_q.

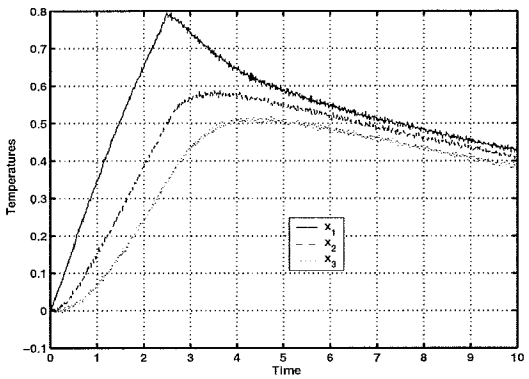

Figure 2. Temperature measurements ($\sigma = 0.01$).

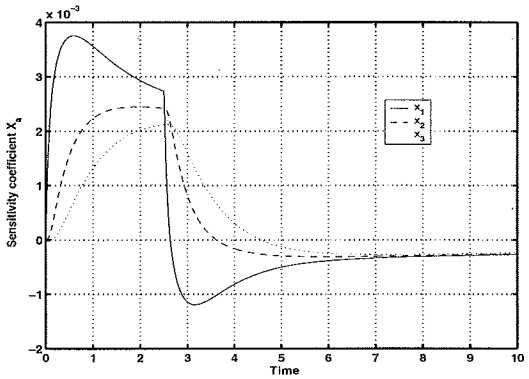

Figure 3. Sensitivity coefficient X_a as time function.

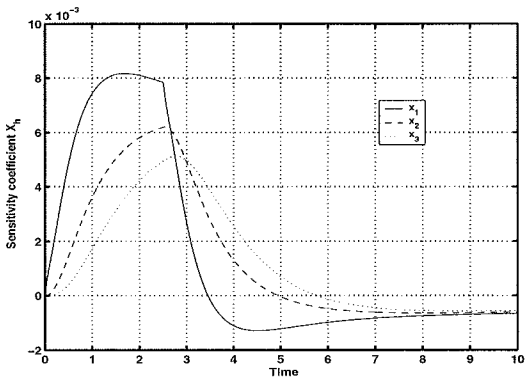

Figure 4. Sensitivity coefficient X_h as time function.

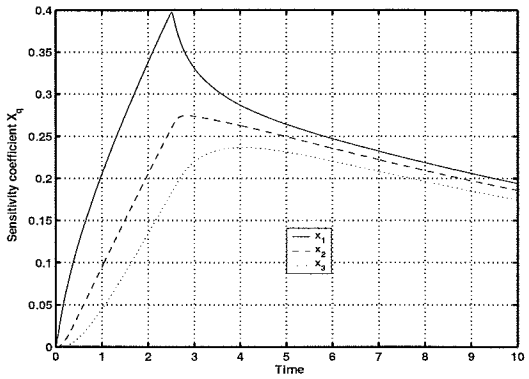

Figure 5. Sensitivity coefficient X_q as time function.

The sensitivity X_q has the same time evolution as measurements but with a half value in amplitude. The sensitivity X_a and X_h present approximately the same time evolution, however with a maximum value 1000 times lower than the temperature measurements. The amplitude of Xh is twice, as important as the one of X_a. To inspect, the linearity between X_a and Xh we have plotted the time function of the ratio X_a/X_h in Figure 6. A carefully examination of this ratio, shows a non-constant value between them but presents an abrupt change around

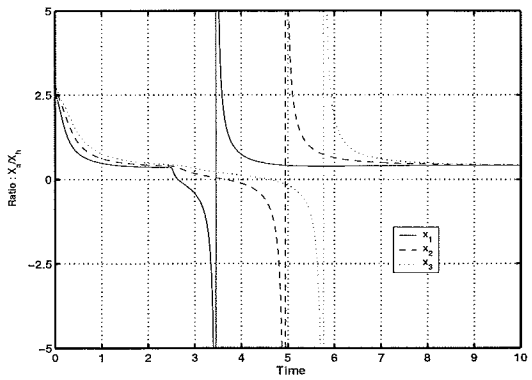

Figure 6. The ration X_a/X_h as time function.

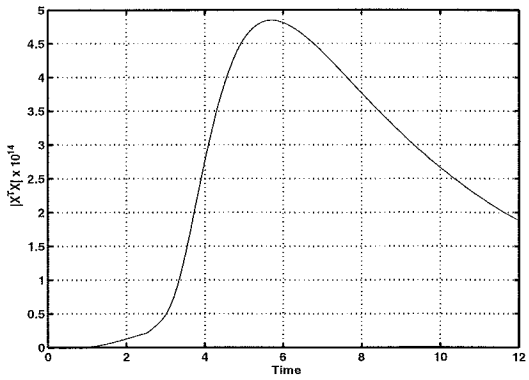

Figure 7. Determinant $|X^TX|$ as time function.

the end of the heating time, .i.e $t_h = 2.50$. This means that there is a relatively wide room, around this time, to estimate simultaneously these three parameters.

Figure 7 shows the variation of the determinant of $\mathbf{X}^T\mathbf{X}$ as a function of time. An analysis of this figure reveals that, for three sensors located at $x_1 = 2$, $x_2 = 4$, and $x_3 = 6$, and a heating time as $t_h = 2.5$, the duration of the experiment should be taken at least as far as $t_f = 5.7$ where such determinant is maximum, so that the confidence region of estimated parameters is minimized.

The above analysis was accomplished by considering fixed values of a, h, and q. However, in practical welding, there is a big change in all of them and seeing the dependence between them, how the sensitivity coefficients vary if the three parameters undergo a variation. To answer this question, we have plotted different 3-D graphs showing the change in the reduced sensitivity with one parameter while the two others are kept constant. As they present the same behavior, for any given sensors location, this analysis is performed only for the first sensor located at x_1. The results are summarized in Figures 8-15. For the sake of the limitation length of this paper, we can just conclude that there is no linearity between a, h, and q and all of them could be estimated at the same time.

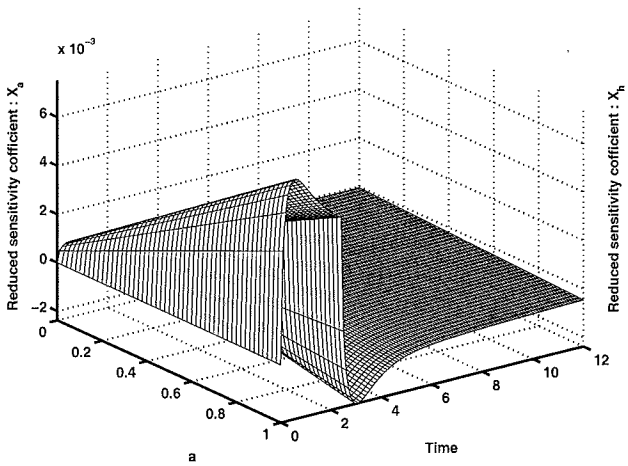

Figure 8. Sensitivity coefficient X_a as function of time and a.

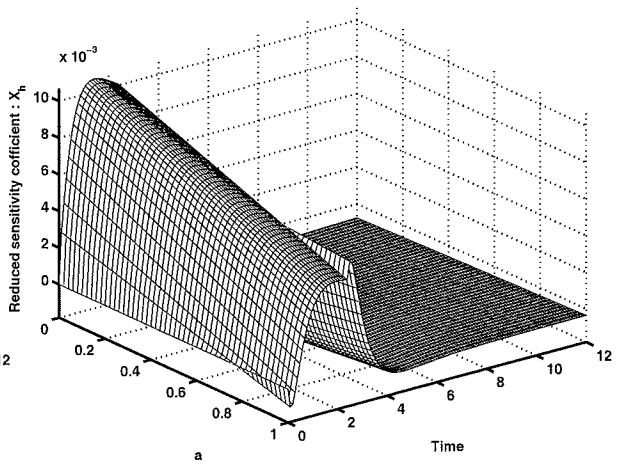

Figure 9. Sensitivity coefficient X_h as function of time and a.

In what follows, we consider the estimation of a, h, and q, by using 1200 transient temperature histories of three sensors located at $x_1 = 2$, $x_2 = 4$, and $x_3 = 6$. Measurements with different levels of random error were considered for the analysis, including $\sigma = 0$ (errorless measurements) and $\sigma = 0.004T_m$, where T_m is the maximum measured temperature at x_1. For the estimation of the unknown parameters, we utilized the Levenberg-Marquardt method of minimization of the least squares norm. The subroutine DBCLSJ of IMSL [8, 13], based on a such method, was used in the present work. The results shown below, obtained with measurements with random error, were averaged over 100 runs in order to reduce the bias introduced by the random number generator utilized [3].

The simulated transient temperature data $Y(x_i, t_j)$ containing measurement errors are generated by adding random errors to the computed exact temperatures $T(x_i, t_j)$ as follow :

$$Y(x_i, t_j) = T(x_i, t_j) + \sigma\,\omega \qquad i = 1, \ldots, N_s, \qquad j = 1, \ldots, N_t \tag{19}$$

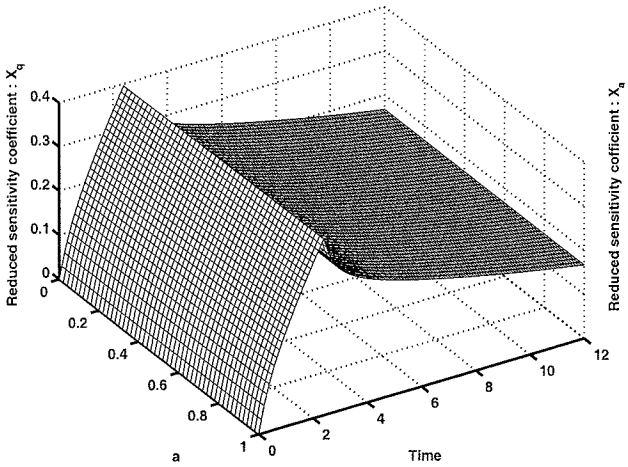

Figure 10. Sensitivity coefficient X_q as function of time and a.

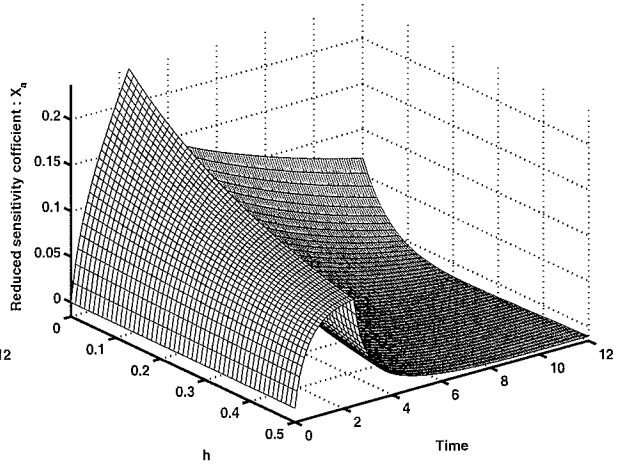

Figure 11. Sensitivity coefficient X_a as function of time and h. $h \in [0.01,\ 0.5]$.

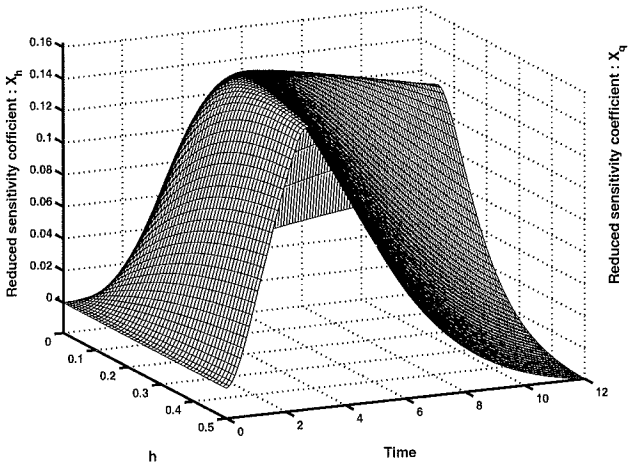

Figure 12. Sensitivity coefficient X_h as function of time and h. $h \in [0.01,\ 0.5]$.

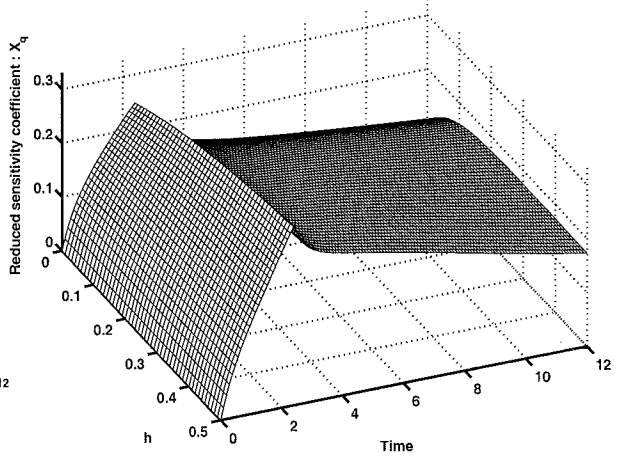

Figure 13. Sensitivity coefficient X_q as function of time and h. $h \in [0.01,\ 0.5]$.

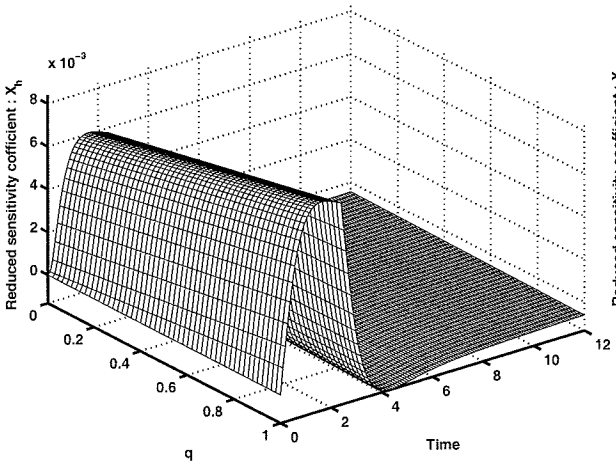

Figure 14. Sensitivity coefficient X_h as function of time and q.

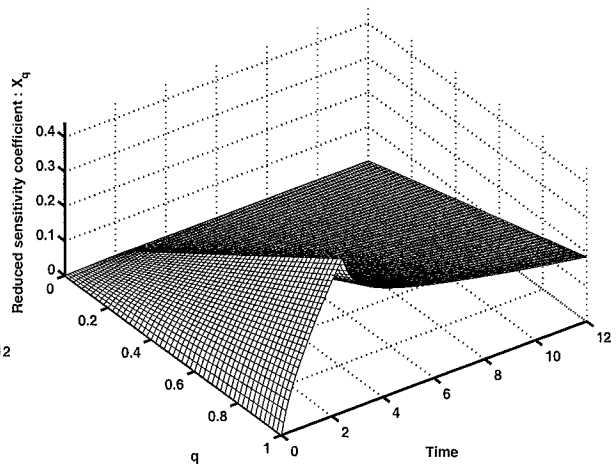

Figure 15. Sensitivity coefficient X_q as function of time and q.

where σ is the standard deviation of the measurement errors which is assumed to be the same for all measurements, N_s is the number of sensors, and N_t is the number of measurements taken with each sensor i. For normally distributed random errors, there is a 99 % probability of the value of ω lying in the range $-2.576 < \omega < +2.576$. The values ω are generated randomly by the IMSL subroutine DRNNOR [8]. To quantify the relative error of the

estimation procedure, the following definition is introduced

$$\varepsilon_i = \left| \frac{u_i - \bar{u}_i}{\bar{u}_i} \right| \times 100\% \qquad i = 1, 2, 3 \tag{20}$$

is the estimation error for the parameter under hand and the over-bar designates its exact value.

Table 1. Estimated parameters and confidence intervals obtained with $t_h = 2.5$ and $t_f = 12.5$.

Test case	Parameter u_i	Exact value	Initial guess ($k = 0$)	Estimated $\sigma = 0$	Estimated $\sigma = 0.004 T_m$	Standard deviation	Error ε_i (%)
1	a	0.5000	0.01	0.5000	0.4994	0.1173	0.110
	h	0.0222	0.01	0.0222	0.0222	0.0038	0.102
	q	0.8989	0.01	0.8989	0.9005	0.2099	0.180
2	a	0.5000	0.01	0.5000	0.5000	0.0020	0.004
	h	0.2222	0.01	0.2222	0.2222	0.0014	0.020
	q	0.8989	0.01	0.8989	0.8987	0.0028	0.009
3	a	0.5000	0.01	0.5000	0.5005	0.0149	0.113
	h	2.222	0.01	2.222	2.2199	0.0333	0.100
	q	0.8989	0.01	0.8989	0.8989	0.0008	0.002
4	a	0.5000	0.01	0.5000	0.4958	0.1663	0.833
	h	22.222	0.01	22.222	22.290	3.3962	0.307
	q	0.8989	0.01	0.8989	0.8988	0.0008	0.002

Table 1 summarizes the results obtained for the estimated parameters with different test-cases. The presented results were obtained with $\Delta Fo = 0.08$. It is shown that the heat flux generated by the Joule effect, the thermal conductance, and the intrinsic heat partition coefficient are not so correlated as mentioned elsewhere [10], and can be estimated simultaneously under the following conditions : (1) at least one sensor should be installed in the electrode tip as close as possible to the interface but without disturbing the constriction effect taking place in the vicinity of the interface, (2) the boundary condition of the electrode tip is preferred to be of the third kind (Newton condition), (3) the final time experiment should be at least two times and half of the heating time (period of current flow), and (4) this method remains applicable for wide range of dimensionless thermal properties, i.e. different values of α and k. In other words, this method is still working with other couples of materials, in electrical and thermal contact, provided that there is a joule effect in both regions and their common interface.

8. CONCLUSIONS

This paper shows the application of the Levenberg-Marquardt method to estimate simultaneously three thermo-physical parameters needed in characterizing the thermal behavior of thermo-electrical contact. The presented results show that the simultaneously estimation is feasible besides the relatively high degree of correlation among of these parameters. The presentation of the results in dimensionless form allows the analysis of a wide range of different materials in such complicated environment. The study shows that the agreements between the estimated and exact parameters are reasonable even when parameter estimation is performed with high noised data.

The more realistic problem would be the estimation of the same unknowns as time function. In fact, the heat flux released at the interface and its partition coefficient as well as the thermal contact conductance between the two solids in electrical and thermal contact evolve in dynamic environment and depend strongly on time and temperature. This problem is quite different than the one presented in this study in the sense that it deals with the simultaneously estimation of three time or temperature dependent functions. This kind of problem is more difficult because it concerns the estimation of an infinite number of parameters at once. The resolution of such problem by means of function estimation tools is currently underway and will be published nextly. Also, optimization of the experimental design setup and the use of experimental data will be considered.

REFERENCES

1. American Welding Society, Resistance and solid state welding and other joining processes. *Welding Handbook* (1980) **3**,1-55.

2. J.G. Bauzin and N. Laraqi, Simultaneously estimation of frictional heat flux and two thermal contact parameters for sliding contacts. *Numerical Heat Transfer : Part A, Applications* (2003) **45**(3),313-328.

3. J.V. Beck and K.J. Arnold, *Parameter Estimation in Engineering and Science*, Wiley Interscience, New York, 1977.

4. F.P. Bowden and J.P.B. Williamson, Electrical conduction in solids. Influence of the passage of current on the contact between solids. *Proc. Roy. Soc. London* (1959) **246**,1-12.

5. L.S. Fletcher, Recent Developments in Contact Conductance Heat Transfer. *ASME, J. Heat Transfer* (1988) **110**,1059-1070.

6. J.A. Greenwood, Temperatures in spot welding, *British Welding J.* (1961) **8**(6),316-322.

7. R. Holm, *Electric contacts*, Springer-Verlag, Berlin, 1967.

8. IMSL, *Library Edition 10.0, User's Manual, Math/Library*, Houston, Texas, USA, 1987.

9. J.C. Jeager, Moving sources of heat and the temperature at sliding contacts. *Proc. Roy. N. South. W.* (1942) **56**,203-223.

10. G. Le Meur, *Etude de la Condition de Liaison Thermique à une Interface de Contact Solide-Solide Siège d'une Dissipation par Effet Joule : Application au Soudage par Point*, PhD thesis, Univesité de Nantes, Nantes, France, December, 2002.

11. T. Loulou and J.P. Bardon, Estimation of thermal contact conductance during resistance spot welding. *Experimental Heat Transfer* (2001) **14**,251-264.

12. C.V. Madhusudana, *Thermal Contact Conductance*, Springer-Verlag, New York, 1995.

13. J.J. Moré, The Levenberg-Marquardt algorithm : Implementation and theory, *Numerical Analysis, Lectures Notes in Mathematics*, (eds. G.A. Watson), Springer Verlag, Berlin, 1977, **630**, pp.105-116.

14. M.N. Ozişik and H.R.B. Orlande, *Inverse Heat Transfer : Fundamentals and Applications*, Taylor and Francis, Pennsylvania, 1999.

15. E. Polak, *Computational Methods in Optimization*, Academic Press, New York, 1971.

16. W. Rice and E.J. Funck, An analytical investigation of the temperature distribution during resistance welding. *Welding J.* (1961) **46**(4),175-186.